Structural Engineering and Mechanics, *Vol. 54, No. 3 (2015) 419-432*
DOI: http://dx.doi.org/10.12989/sem.2015.54.3.419

AMDM for free vibration analysis of rotating tapered beams

Qibo Mao*

School of Aircraft Engineering, Nanchang HangKong University, 696 South Fenghe Avenue, Nanchang, CN-330063, P.R. China

(Received March 30, 2014, Revised October 9, 2014, Accepted October 28, 2014)

Abstract. The free vibration of rotating Euler-Bernoulli beams with the thickness and/or width of the cross-section vary linearly along the length is investigated by using the Adomian modified decomposition method (AMDM). Based on the AMDM, the governing differential equation for the rotating tapered beam becomes a recursive algebraic equation. By using the boundary condition equations, the dimensionless natural frequencies and the closed form series solution of the corresponding mode shapes can be easily obtained simultaneously. The computed results for different taper ratios as well as different offset length and rotational speeds are presented in several tables and figures. The accuracy is assured from the convergence and comparison with the previous published results. It is shown that the AMDM provides an accurate and straightforward method of free vibration analysis of rotating tapered beams.

Keywords: adomian modified decomposition method; rotating tapered beam; taper ratio; natural frequency; mode shape

1. Introduction

The determination of natural frequencies and mode shapes of rotating tapered beams is very important for the design of helicopter blades, airplane propellers and wind turbines etc. As a result, the free vibration analysis of rotating tapered beams has been extensively studied by many researchers with great success. For examples, the publications (Banerjee 2000, Banerjee *et al.* 2006, Banerjeea and Jackson 2013) used the dynamic stiffness method based on Frobenius solutions to solve the free bending vibration of the uniform and tapered rotating beam. The publications (Wang and Wereley 2004, Vinod *et al.* 2007) imposed spectral finite element method for vibration analysis of rotating blades with uniform tapers under cantilever and hinged boundary conditions. The publications (Ozdemir and Kaya 2006a, b, Rajasekaran 2013) applied differential transformation method (DTM) for the free vibration analysis of tapered rotating beams. Bazoune (2007) discussed the effect of taper ratio on the natural frequencies of the beam using finite element method.

Recently, a relatively new computed approach called Adomian modified decomposition method (AMDM) (Adomian 1994) has been applied to the free vibration problem for several beam structures, such as linear and nonlinear tapered beam under general boundary conditions (Hsu *et*

*Corresponding author, Professor, E-mail: qibo_mao@yahoo.com

http://www.techno-press.org/?journal=sem&subpage=8 ISSN: 1225-4568 (Print), 1598-6217 (Online)

al. 2008, Mao and Pietrzko 2012), multiple-stepped beams (Mao 2011), elastically connected multiple-beam systems (Mao 2012) and uniform rotating beam (Mao 2013). The AMDM has shown reliable results in providing analytical approximation that converges rapidly (Adomian 1994). In this study, the AMDM is extended to analyze the free vibration for the rotating tapered Euler-Bernoulli beams under various taper ratios, rotating speeds and offset lengths. The AMDM is a straightforward and powerful method for solving linear and nonlinear differential equations. The main advantages of AMDM are computational simplicity and do not involve any linearization, discretization, perturbation. In AMDM the solution is considered as a sum of an infinite series, and rapid convergence to an accurate solution.

Using the AMDM, the governing differential equation for the rotating tapered beam becomes a recursive algebraic equation. The boundary conditions become simple algebraic frequency equations which are suitable for symbolic computation. Moreover, after some simple algebraic operations on these frequency equations, the natural frequency and corresponding closed-form series solution of mode shape can be determined simultaneously. Finally, the effects of the taper ratios, rotating speeds and offset lengths on the natural frequencies and mode shapes are investigated. The results are compared with previous published ones to demonstrate the accuracy and efficiency of the proposed method.

2. AMDM for the rotating beams

Consider the free vibration of a rotating tapered cantilever Euler-Bernoulli beam with length L, both continuously linearly varying width $b(x)$ and thickness $h(x)$, as shown in Fig. 1. The variation of the width and thickness along beam length L are defined as

$$b(x) = b_0\left(1 - c_b \frac{x}{L}\right), \quad h(x) = h_0\left(1 - c_h \frac{x}{L}\right) \tag{1}$$

where b_0 and h_0 are the width and thickness at the root of the beam, respectively. c_b and c_h are the width and thickness taper ratios, respectively.

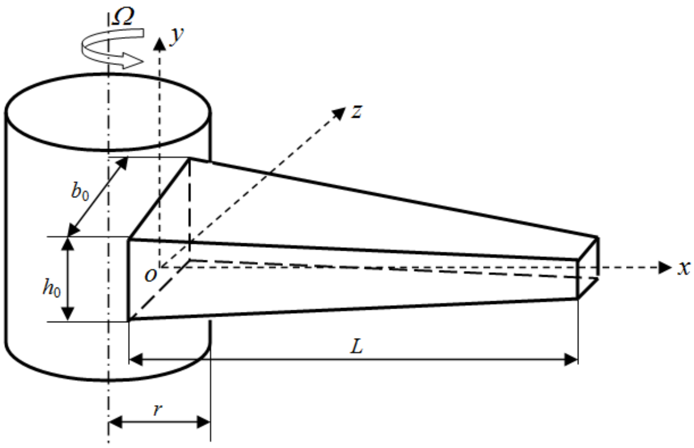

Fig. 1 A rotating tapered cantilever Euler-Bernoulli beam

The partial differential equation describing the out-of-plane bending vibration of a rotating tapered beam is as follows (Banerjee *et al*. 2006, Wang and Wereley 2004)

$$\frac{\partial^2}{\partial x^2}\left[EI(x)\frac{\partial^2 w(x,t)}{\partial x^2}\right]+\rho A(x)\frac{\partial^2 w(x,t)}{\partial t^2}-\frac{\partial}{\partial x}\left[T(x)\frac{\partial w(x,t)}{\partial x}\right]=0 \tag{2}$$

where E and ρ are Young's modulus and the density of the beam, respectively. $A(x)$ and and $I(x)$ are the cross-sectional area and the cross-sectional moment of inertia of the beam, respectively.

$$A(x)=b(x)h(x)=A_0\left(1-c_b\frac{x}{L}-c_h\frac{x}{L}+c_bc_h\frac{x^2}{L^2}\right) \tag{3}$$

$$I(x)=\frac{b(x)h^3(x)}{12}=I_0\left(1-c_b\frac{x}{L}\right)\left(1-c_h\frac{x}{L}\right)^3=I_0\left(1+\alpha_1\frac{x}{L}+\alpha_2\frac{x^2}{L^2}+\alpha_3\frac{x^3}{L^3}+\alpha_4\frac{x^4}{L^4}\right) \tag{4}$$

where $A_0=b_0h_0$, $I_0=\frac{b_0h_0^3}{12}$, $\alpha_1=-(c_b+3c_h)$, $\alpha_2=3c_h(c_b+c_h)$, $\alpha_3=-c_h^2(3c_b+c_h)$, $\alpha_4=c_bc_h^3$.

$T(x)$ in Eq. (2) is the axial force due to the centrifugal stiffening and is given by the following (Banerjee *et al*. 2006, Wang and Wereley 2004)

$$T(x)=\int_x^L\left[\rho A(x)\Omega^2(r+x)\right]dx \tag{5}$$

where Ω is the angular rotating speed of the beam, r is offset length between beam and rotating hub.

According to modal analysis approach (For harmonic free vibration), the $w(x,t)$ can be separated in space and time

$$w(x,t)=\phi(x)e^{i\omega t} \tag{6}$$

where $i=\sqrt{-1}$, $\phi(x)$ and ω are the structural mode shape and the natural frequency, respectively.

Substituting Eq. (6) into Eq. (2), then separating variable for time t and space x, the ordinary differential equation for the rotating beam can be obtained

$$\begin{aligned}&EI(x)\frac{d^4\phi(x)}{dx^4}+2E\frac{dI(x)}{dx}\frac{d^3\phi(x)}{dx^3}+E\frac{d^2I(x)}{dx^2}\frac{d^2\phi(x)}{dx^2}\\&-T(x)\frac{d^2\phi(x)}{dx^2}-\frac{dT(x)}{dx}\frac{d\phi(x)}{dx}-\rho A(x)\omega^2\phi(x)=0\end{aligned} \tag{7}$$

To rewrite Eqs. (5) and (7) into dimensionless form, we define

$$X=\frac{x}{L},\ R=\frac{r}{L},\ U=\sqrt{\frac{\rho A_0\Omega^2L^4}{EI_0}},\ \Phi(X)=\frac{\phi(x)}{L},\ \lambda=\sqrt{\frac{\rho A_0\omega^2L^4}{EI_0}} \tag{8}$$

where λ is the dimensionless natural frequency, and the nth dimensionless natural frequency is denoted as $\lambda(n)$. U is the dimensionless rotating speed of the beam.

Substituting Eq. (4) into Eq. (5), the axial force $T(x)$ within a rotating beam can be expressed as

$$T(x)=\frac{EI_0}{L^4}U^2\left(\beta_0+\beta_1\frac{x}{L}+\beta_2\frac{x^2}{L^2}+\beta_3\frac{x^3}{L^3}+\beta_4\frac{x^4}{L^4}\right) \tag{9}$$

where $\beta_0=\frac{1}{12}\left[12R+3c_bc_h-4(c_b+c_h-c_bc_hR)+6(1-c_bR-c_hR)\right]$, $\beta_1=-R$,

$\beta_2=-\frac{1}{2}(c_bR+c_hR-1)$, $\beta_3=\frac{1}{3}(c_b+c_h-c_bc_hR)$, $\beta_4=-\frac{c_bc_h}{4}$.

Substituting Eqs. (4) and (9) into Eq. (7), then rewrite Eq. (7) in dimensionless form

$$\begin{aligned}&\left(1+\alpha_1X+\alpha_2X^2+\alpha_3X^3+\alpha_4X^4\right)\frac{d^4\Phi(X)}{dX^4}+2\left(\alpha_1+2\alpha_2X+3\alpha_3X^2+4\alpha_4X^3\right)\frac{d^3\Phi(X)}{dX^3}\\&+\left(2\alpha_2+6\alpha_3X+12\alpha_4X^2\right)\frac{d^2\Phi(X)}{dX^2}-U^2\left(\beta_0+\beta_1X+\beta_2X^2+\beta_3X^3+\beta_4X^4\right)\frac{d^2\Phi(X)}{dX^2}\\&-U^2\left(\beta_1+2\beta_2X+3\beta_3X^2+4\beta_4X^3\right)\frac{d\Phi(X)}{dX}-\lambda^2\left(1-c_bX-c_hX+c_bc_hX^2\right)\Phi(X)=0\end{aligned} \tag{10}$$

According to the AMDM (Adomian 1994, Hsu *et al.* 2008, Mao 2012, 2013), $\Phi(X)$ in Eq. (10) can be expressed as an infinite series

$$\Phi(X)=\sum_{m=0}^{\infty}C_mX^m \tag{11}$$

where the unknown coefficients C_m will be determined recurrently.

Impose a linear operator $G=\frac{d^4}{dX^4}$, then the inverse operator of G is therefore a 4-fold integral operator defined by

$$G^{-1}=\int_0^x\int_0^x\int_0^x\int_0^x(\ldots)dXdXdXdX \tag{12}$$

and

$$G^{-1}G[\Phi(X)]=\Phi(X)-C_0-C_1X-C_2X^2-C_3X^3 \tag{13}$$

Applying both sides of Eq. (10) with G^{-1}, we get

$$\begin{aligned}G^{-1}G[\Phi(X)]=G^{-1}\Bigg[&-\left(\alpha_1X+\alpha_2X^2+\alpha_3X^3+\alpha_4X^4\right)\frac{d^4\Phi(X)}{dX^4}\\&-2\left(\alpha_1+2\alpha_2X+3\alpha_3X^2+4\alpha_4X^3\right)\frac{d^3\Phi(X)}{dX^3}\\&-\left(2\alpha_2+6\alpha_3X+12\alpha_4X^2\right)\frac{d^2\Phi(X)}{dX^2}\end{aligned}$$

$$\begin{aligned}&+U^2\left(\beta_0+\beta_1 X+\beta_2 X^2+\beta_3 X^3+\beta_4 X^4\right)\frac{d^2\Phi(X)}{dX^2}\\&+U^2\left(\beta_1+2\beta_2 X+3\beta_3 X^2+4\beta_4 X^3\right)\frac{d\Phi(X)}{dX}\\&+\lambda^2\left(1-c_b X-c_h X+c_b c_h X^2\right)\Phi(X)\Big]\end{aligned} \tag{14}$$

Substituting Eqs. (11) and (13) into Eq. (14), we get

$$\Phi(X)=\sum_{m=0}^{3}C_m X^m+\sum_{m=0}^{\infty}D_m X^{m+4}+\sum_{m=0}^{\infty}E_m X^{m+5}+\sum_{m=0}^{\infty}F_m X^{m+6} \tag{15}$$

And

$$\begin{aligned}D_m=&\frac{\lambda^2-(m-1)m(m+1)(m+2)\alpha_4+m(m+1)U^2\beta_2}{(m+1)(m+2)(m+3)(m+4)}C_m\\&+\frac{-m(m+1)(m+2)\alpha_3+(m+1)U^2\beta_1}{(m+2)(m+3)(m+4)}C_{m+1}\\&+\frac{-(m+1)(m+2)\alpha_2+U^2\beta_0}{(m+3)(m+4)}C_{m+2}-\frac{\alpha_1(m+2)}{(m+4)}C_{m+3}\end{aligned} \tag{16}$$

$$E_m=\frac{-(c_b+c_h)\lambda^2+m(m+2)U^2\beta_3}{(m+1)(m+2)(m+3)(m+4)}C_m \tag{17}$$

$$F_m=\frac{c_b c_h\lambda^2+m(m+1)U^2\beta_4}{(m+1)(m+2)(m+3)(m+4)}C_m \tag{18}$$

Comparing Eq. (11) to Eq. (15), the coefficients C_m (m>4) in Eq. (11) can be determined by using the following recurrence relations

$$C_{m+4}=\begin{cases}D_m & m=0\\ D_m+E_{m-1} & m=1\\ D_m+E_{m-1}+F_{m-2} & m\geq 2\end{cases} \tag{19}$$

We may approximate the above solution by the M-term truncated series, Eq.(11) can be rewritten as

$$\Phi(X)=\sum_{m=0}^{M}C_m X^m \tag{20}$$

Eq. (20) implies that $\sum_{m=M+1}^{\infty}C_m X^m$ is negligibly small. The number of the series summation limit M is determined by convergence requirement in practice.

From above analysis, it can be found that there are five unknown parameters (C_0, C_1, C_2, C_3 and λ) for the free vibration analysis of the rotating beam. These unknown parameters can be determined by using the boundary condition equations of the beam, and then the natural frequencies and corresponding mode shapes for the rotating beams can be obtained.

3. Natural frequencies and mode shapes

The cantilevered boundary conditions of the rotating beam shown in Fig. 1 can be expressed into dimensionless form (Banerjee 2000, Banerjee *et al.* 2006, Wang and Wereley 2004), wet get

$$\Phi(0) = \frac{d\Phi(0)}{dX} = 0 \tag{21}$$

$$\frac{d^2\Phi(1)}{dX^2} = \frac{d^3\Phi(1)}{dX^3} = 0 \tag{22}$$

Substituting Eq. (20) into Eqs. (21) and (22), we get

$$C_0 = 0\,,\ C_1 = 0 \tag{23}$$

According to Eq. (20), the second and third spatial derivative of the mode shapes can be expressed as

$$\frac{d^2\Phi(X)}{dX^2} = \sum_{m=0}^{M-2}(m+1)(m+2)C_{m+2}X^m \tag{24}$$

$$\frac{d^3\Phi(X)}{dX^3} = \sum_{m=0}^{M-3}(m+1)(m+2)(m+3)C_{m+3}X^m \tag{25}$$

By using Eqs. (24) and (25), Eq. (22) can be expressed as

$$\frac{d^2\Phi(1)}{dX^2} = \sum_{m=0}^{M-2}(m+1)(m+2)C_{m+2} = 2C_2 + 6C_3 + 12C_4 + 20C_5 + 30C_6 + 42C_7 + \ldots = 0 \tag{26}$$

$$\frac{d^3\Phi(1)}{dX^3} = \sum_{m=0}^{M-3}(m+1)(m+2)(m+3)C_{m+3} = 6C_3 + 24C_4 + 60C_5 + 120C_6 + 210C_7 + \ldots = 0 \tag{27}$$

Substituting Eqs. (16)-(19) and (23) into Eqs. (26) and (27), C_m (m>3) in Eqs. (26) and (27) can be expressed as linear functions of C_2 and C_3 through a recursive way. It means that there are only three unknown parameters (C_2, C_3 and λ) in Eqs. (26) and (27). So these two boundary condition equations can be expressed as

$$\frac{d^2\Phi(1)}{dX^2} = f_{11}(\lambda)C_2 + f_{12}(\lambda)C_3 = 0 \tag{28}$$

$$\frac{d^3\Phi(1)}{dX^3} = f_{21}(\lambda)C_2 + f_{22}(\lambda)C_3 = 0 \tag{29}$$

Table 1 The convergence of the dimensionless natural frequencies $\lambda(n)$ for a tapered beam (U=12, R=0, c_b=0, c_h=0.5)

M	Mode index			
	1	2	3	4
10	26.495055041695	40.536930048779	75.300698302519	206.053571179223
20	13.452009966574	33.995750398931	64.602868940583	108.008955209130
30	13.470052122327	34.038087943671	65.509436018609	110.430372129048
40	13.471236306204	34.093487129711	65.533042916599	110.218531535904
50	13.471129006455	34.087677953868	65.523660855132	110.225006691375
60	13.471129934581	34.087674922285	65.523664134660	110.225008319294
70	13.471129933314	34.087674923875	65.523654261033	110.225008006113
80	13.471129933318	34.087674923877	65.523654261717	110.225008006927
90	13.471129933314	34.087674923685	65.523654261270	110.225008006227
100	13.471129933314	34.087674923682	65.523654261246	110.225008006567
	13.4711[a]	**34.0877** [a]	**65.5237** [a]	**N/A.**

[a]Results from Wang and Wereley (2004)

The explicit forms for f_{ij} in Eqs. (28) and (29) are very complex. However, all the algebraic calculations are finished quickly using symbolic computational software (such as MATLAB).

From Eqs. (28) and (29), the nth dimensionless frequency parameter $\lambda(n)$ can be solved by

$$f_{11}(\lambda)f_{22}(\lambda)-f_{12}(\lambda)f_{21}(\lambda)=\sum_{n=0}^{N}S_n\lambda^n=0 \tag{30}$$

Notice that Eq. (30) is a polynomial of degree N evaluated at λ. By using the functions **sym2poly** and **roots** in MATLAB Symbolic Math Toolbox, Eq. (30) can be directly solved. The next step is to determine the nth mode shape function corresponding to nth dimensionless frequency $\lambda(n)$. Substituting the solved $\lambda(n)$ into Eqs. (28) or (29), then C_3 can be expressed as the function of C_2.

$$C_3=-\frac{f_{11}(\lambda)}{f_{12}(\lambda)}C_2=-\frac{f_{21}(\lambda)}{f_{22}(\lambda)}C_2 \tag{31}$$

Substituting solved C_0, C_1, C_2, C_3 and $\lambda(n)$ into equations. Eqs. (16)-(18) and using Eq. (19), all other coefficients C_{m+4} ($m\geq 0$) can be determined. Then the corresponding nth mode shape function can be obtained by using Eq. (20).

4 Numerical calculations

In order to verify the proposed method to analyze the free vibration of the rotating tapered beam shown in Fig. 1, several numerical examples will be discussed in this section.

As mentioned earlier, the closed-form series solutions of mode shape functions in Eq. (20) will have to be truncated in numerical calculations. It is important to check how rapidly the dimensionless natural frequencies $\lambda(n)$ computed through AMDM converge toward the exact

Table 2 The first five dimensionless natural frequencies $\lambda(n)$ for a beam with different dimensionless rotating speed U and offset length R when taper ratios c_b=0 and c_h=0.5

R	U	Mode index n				
		1	2	3	4	5
0	0	3.823785	18.317261	47.264827	90.450478	148.001745
		3.82379 [a]	**18.3173** [a]	**47.2648** [a]	**90.4505** [a]	**148.002** [a]
	1	3.986618	18.474006	47.417284	90.603916	148.156266
		3.98661 [a]	**18.4740** [a]	**47.4173** [a]	**90.6039** [a]	**148.156** [a]
	5	6.743399	21.905325	50.933807	94.206358	151.814249
		6.74340 [a]	**21.9053** [a]	**50.9338** [a]	**94.2064** [a]	**151.814** [a]
	10	11.501549	30.182744	60.563880	104.611993	162.677340
		11.5015 [a]	**30.1827** [a]	**60.5639** [a]	**104.612** [a]	**162.677** [a]
	12	13.471130	34.087675	65.523654	110.225008	168.698805
		13.4711 [b]	**34.0877** [b]	**65.5237** [b]	**N/A.**	**N/A.**
0.5	1	4.090409	18.576241	47.521021	90.710782	148.265331
		4.09041 [c]	**18.5762** [c]	**47.521** [c]	**90.7108** [c]	**N/A.**
	2	4.797840	19.332499	48.280957	91.486873	149.053055
		4.79784 [c]	**19.3325** [c]	**48.281** [c]	**91.4869** [c]	**N/A.**
	3	5.777354	20.531144	49.520040	92.764695	150.355963
		5.77735	***20.5311***	***49.520***	***92.7647***	***N/A.***
	4	6.905011	22.099559	51.201280	94.522100	152.159643
		6.90501 [c]	**22.0996** [c]	**51.2013** [c]	**94.5221** [c]	**N/A.**
	5	8.112317	23.963571	53.279988	96.730532	154.444926
	10	14.550041	35.830843	68.033704	113.328854	172.206341
1	1	4.191561	18.677904	47.624510	90.817507	148.374307
		4.19156 [c]	**18.6779** [c]	**47.6245** [c]	**90.8175** [c]	**N/A.**
	2	5.132800	19.720216	48.686515	91.908976	149.485898
		5.1328 [c]	**19.7202** [c]	**48.6865** [c]	**91.9090** [c]	**N/A.**
	3	6.386783	21.343711	50.403352	93.697163	151.318673
		6.38678 [c]	**21.3437** [c]	**50.4034** [c]	**93.6972** [c]	***N/A.***
	4	7.793079	23.425519	52.706332	96.139351	153.844302
		7.79308 [c]	**23.4255** [c]	**52.7063** [c]	**96.1394** [c]	**N/A.**
	5	9.275320	25.851548	55.516746	99.182173	157.025860
	10	17.047961	40.660692	74.676635	121.331238	181.161248
2	1	4.386682	18.879550	47.830751	91.030537	148.591990
		4.38668 [c]	**18.8795** [c]	**47.8308** [c]	**91.0305** [c]	**N/A.**
	2	5.742591	20.473019	49.486678	92.746713	150.347390
		5.74259 [c]	**20.473** [c]	**49.4867** [c]	**92.7467** [c]	**N/A.**
	3	7.452740	22.879476	52.120555	95.531374	153.223681
		7.45274 [c]	**22.8795** [c]	**52.1206** [c]	**95.5314** [c]	**N/A.**
	4	9.310318	25.866257	55.581704	99.284677	157.152488
		9.31032 [c]	**25.8663** [c]	**55.5817** [c]	**99.2847** [c]	**N/A.**
	5	11.234823	29.248242	59.713029	103.889078	162.048101
	10	21.156567	48.841444	86.280212	135.724961	197.672644

[a]Results from Banerjee *et al.* (2006)
[b]Results from Wang and Wereley (2004)
[c]Results from Ozdemir and Kaya (2006b)

Table 3 The first five dimensionless natural frequencies $\lambda(n)$ for a tapered beam with different dimensionless rotating speed U and offset length R when taper ratios c_b=c_h=0.5

R	U	Mode index n				
		1	2	3	4	5
0	0	4.625150	19.547613	48.578899	91.812768	149.389914
		4.62515 [a]	**19.5476** [a]	**48.5789** [a]	**91.8128** [a]	**149.390** [a]
	1	4.764053	19.680336	48.707343	91.940946	149.518351
		4.76405 [a]	**19.6803** [a]	**48.7073** [a]	**91.9409** [a]	**149.518** [a]
	2	5.156415	20.073355	49.090608	92.324357	149.902965
		5.15641 [a]	**20.0733** [a]	**49.0906** [a]	**92.3243** [a]	**149.903** [a]
	5	7.290145	22.635992	51.691808	94.962652	152.566572
		7.29014 [a]	**22.6360** [a]	**51.6918** [a]	**94.9627** [a]	**152.567** [a]
	10	11.941488	30.029893	60.039884	103.809834	161.700572
		11.9415 [b]	**30.0299** [b]	**60.0399** [b]	**103.810** [b]	**161.701** [b]
1	1	4.945145	19.856664	48.884979	92.122548	149.702951
	2	5.795338	20.756249	49.791371	93.045254	150.637870
	5	9.794041	26.194609	55.704367	99.246969	157.014783
	10	17.600101	39.857367	72.822931	118.589459	177.787425
2	1	5.119662	20.031412	49.061923	92.303758	149.887302
	2	6.368664	21.416902	50.481660	93.760064	151.368853
	5	11.762285	29.309358	59.424681	103.335376	161.327475
	10	21.806335	47.618456	83.510951	131.533983	192.375077
3	1	5.288261	20.204620	49.238183	92.484579	150.071403
	2	6.892955	22.057301	51.161912	94.468930	152.095971
	5	13.436296	32.111656	62.906675	107.251026	165.515375
	10	25.307513	54.236272	92.873277	143.173631	205.797707

[a]Results from Banerjee *et al.* (2006)
[b]Results from Banerjeea and Jackson (2013)

value as the series summation limit M is increased. To examine the convergence of the solution, a beam with dimensionless rotating speed U=12 and dimensionless offset length R=0 is considered. The taper ratios of the beam are assumed as c_b=0 and c_h=0.5. Table 1 shows the dimensionless natural frequencies $\lambda(n)$ as the function of the series summation limit M. Clearly, the $\lambda(n)$ converges very quickly as the series summation limit M is increased. If M=50 is used, the first fourth Ω_1 can be kept accurate to the sixth decimal place. The excellent numerical stability of the solution can also be found in Table 1.

For brief, the series summation limit M in Eq. (20) will be simply truncated to M=60 in all the subsequent calculations. The dimensionless natural frequencies $\lambda(n)$ are kept accurate to the sixth decimal place for comparison purpose. To further check the accuracy of the proposed method, the first five dimensionless natural frequencies $\lambda(n)$ for beams with taper ratios (c_b=0, c_h=0.5) and (c_b=c_h=0.5) under different rotating speeds U and offset lengths R are listed in Tables 2 and 3, respectively. Those calculated results are compared with those listed in the publications (Banerjee *et al.* 2006, Wang and Wereley 2004, Ozdemir and Kaya 2006b) and excellent agreement is found. Due to the stiffening effect of the centrifugal axial force acting on the beam, it can also be found that the natural frequencies increase when the rotating speed or offset length increases, as expected.

Fig. 2 shows the first five mode shapes with different taper ratios and rotating speeds when the offset length R=0. From Fig. 2, it can be found that the discrepancies between the mode shapes under different rotating speeds become smaller as increasing the modal number. However, the natural frequencies are quite different, as shown in Tables 2 and 3.

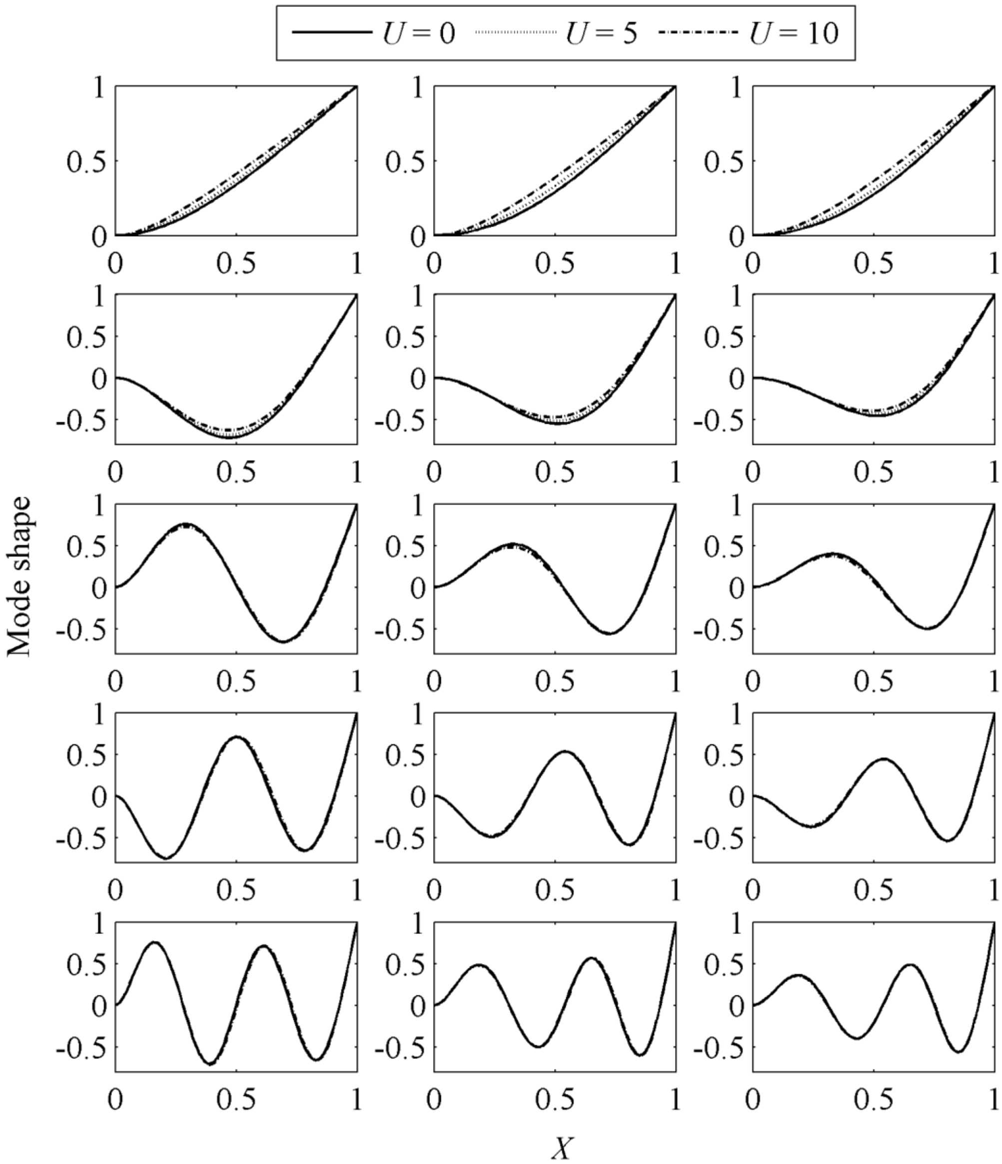

Fig. 2 The first five mode shapes for the rotating tapered beams when offset length R = 0. Columns 1, 2 and 3 are (c_b = c_h =0), (c_b = 0, c_h =0.5) and (c_b = c_b =0.5) respectively. Rows 1, 2, 3, 4 and 5 are the first, second, third, fourth and fifth mode respectively

Table 4 The effect of taper ratios (c_b and c_h) on the dimensionless natural frequencies $\lambda(n)$ for a tapered beam when the dimensionless offset length R=1 and the dimensionless rotating speed U=5

c_h	c_b								
	0	0.1	0.2	0.3	0.4	0.5	0.6	0.7	0.8
(a) The first dimensionless natural frequency $\lambda(1)$									
0	8.940358	9.007297	9.085007	9.176605	9.286602	9.421803	9.593031	9.818689	10.133019
0.1	8.987776	9.055627	9.134327	9.227003	9.338178	9.474670	9.647317	9.874541	10.190608
0.2	9.042467	9.111360	9.191192	9.285099	9.397619	9.535583	9.709845	9.938837	10.256833
0.3	9.106448	9.176547	9.257686	9.353016	9.467089	9.606750	9.782864	10.013868	10.334014
0.4	9.182617	9.254129	9.336801	9.433799	9.549687	9.691329	9.869593	10.102906	10.425454
0.5	9.275320	9.348520	9.433021	9.532005	9.650054	9.794041	9.974835	10.210823	10.536052
0.6	9.391452	9.466714	9.553448	9.654852	9.775524	9.922342	10.10616	10.345274	10.673466
0.7	9.542785	9.620650	9.710194	9.814634	9.938577	10.088896	10.276386	10.519177	10.850535
0.8	9.75160	9.832904	9.926143	10.034548	10.162721	10.317491	10.509519	10.756556	11.090864
(b) The second dimensionless natural frequency $\lambda(2)$									
0	29.352835	29.406757	29.472448	29.554988	29.662650	29.809672	30.022385	30.354322	30.929973
0.1	28.697236	28.747688	28.809182	28.886539	28.987641	29.126107	29.327220	29.642630	30.193119
0.2	28.022082	28.069408	28.127074	28.199644	28.294603	28.424941	28.614871	28.914105	29.439583
0.3	27.324787	27.369416	27.423716	27.491997	27.581350	27.704123	27.883440	28.167016	28.667808
0.4	26.602362	26.644830	26.696356	26.760994	26.845441	26.961405	27.130899	27.399585	27.876284
0.5	25.851548	25.892557	25.942080	26.003930	26.084417	26.194609	26.355400	26.610350	27.063987
0.6	25.069521	25.110009	25.158576	25.218809	25.296653	25.402552	25.556288	25.799290	26.231631
0.7	24.256604	24.297887	24.346985	24.407291	24.484422	24.588246	24.737476	24.971423	25.385544
0.8	23.427109	23.471157	23.523036	23.586008	23.665439	23.770712	23.919568	24.149215	24.550263
(c) The third dimensionless natural frequency $\lambda(3)$									
0	69.760710	69.751504	69.754491	69.776791	69.830202	69.935374	70.131316	70.500248	71.246956
0.1	67.071095	67.064485	67.069251	67.092073	67.144046	67.244648	67.430791	67.780582	68.489564
0.2	64.314844	64.311112	64.317951	64.341593	64.392417	64.488699	64.665203	64.995797	65.666477
0.3	61.480879	61.480366	61.489638	61.514470	61.564510	61.656808	61.823910	62.135312	62.767116
0.4	58.554701	58.557830	58.569983	58.596474	58.646209	58.734973	58.893036	59.185360	59.777753
0.5	55.516746	55.524049	55.539661	55.568428	55.618498	55.704367	55.853949	56.127503	56.680079
0.6	52.339641	52.351826	52.371671	52.403558	52.454870	52.538784	52.680790	52.936254	53.448934
0.7	48.983665	49.001720	49.026906	49.063152	49.117079	49.200537	49.336536	49.575373	50.048849
0.8	45.389145	45.414554	45.446778	45.489319	45.548067	45.633543	45.766207	45.990922	46.426682
(a) The fourth dimensionless natural frequency $\lambda(4)$									
0	129.580326	129.528727	129.489137	129.469822	129.484712	129.558603	129.739159	130.128996	130.992453
0.1	123.867396	123.821470	123.786681	123.770760	123.786767	123.858009	124.029406	124.397968	125.214572
0.2	118.003122	117.963266	117.933688	117.921575	117.939102	118.008048	118.170523	118.517761	119.286765
0.3	111.960553	111.927236	111.903358	111.895556	111.915095	111.982193	112.136062	112.461981	113.182582
0.4	105.703630	105.677415	105.659835	105.656959	105.679129	105.744955	105.890658	106.195345	106.866696
0.5	99.182173	99.163759	99.153218	99.156051	99.181649	99.246969	99.385135	99.668825	100.290073
0.6	92.322688	92.312961	92.310421	92.319987	92.350084	92.415964	92.547534	92.810745	93.381123
0.7	85.009758	85.009901	85.016663	85.034385	85.070509	85.138536	85.265029	85.508861	86.027849
0.8	77.040770	77.052409	77.070287	77.098175	77.142513	77.214969	77.338500	77.564100	78.030314

Table 4 Continued

(a) The fifth dimensionless natural frequency $\lambda(5)$									
0	208.911042	208.834302	208.769584	208.725841	208.718318	208.774471	208.947791	209.355386	210.306328
0.1	199.183559	199.114199	199.055936	199.017133	199.012061	199.066481	199.230699	199.615133	200.512134
0.2	189.189884	189.128354	189.077012	189.043619	189.041453	189.094541	189.249924	189.611145	190.453344
0.3	178.881028	178.827861	178.783995	178.756577	178.757873	178.810130	178.957032	179.295038	180.081492
0.4	168.190791	168.146630	168.110913	168.090167	168.095616	168.147683	168.286589	168.601455	169.331144
0.5	157.025860	156.991493	156.964765	156.951566	156.962058	157.014783	157.146373	157.438316	158.110154
0.6	145.247065	145.223497	145.206837	145.202331	145.219054	145.273603	145.398881	145.668382	146.281271
0.7	132.629758	132.618323	132.613188	132.618953	132.643581	132.701665	132.822207	133.070251	133.623083
0.8	118.7637	118.7662	118.7746	118.7928	118.8277	118.8917	119.0097	119.2373	119.7288

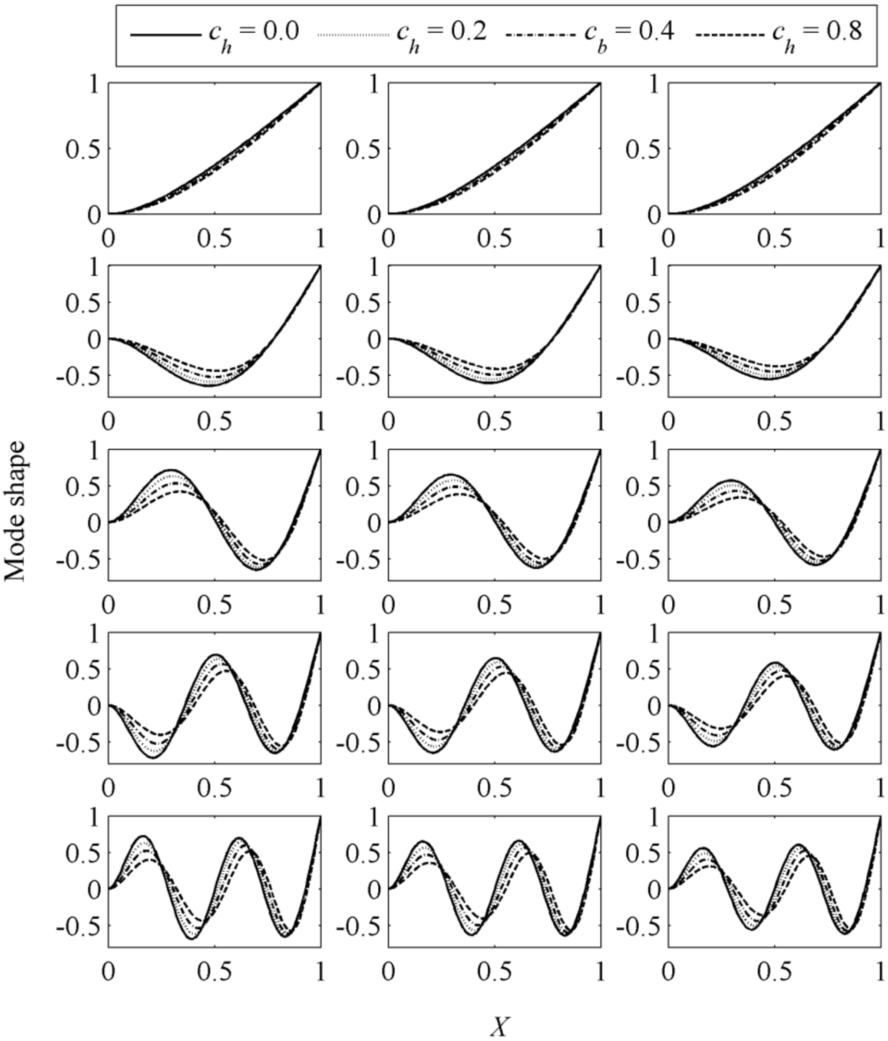

Fig. 3 The first four mode shapes for the rotating beams under different taper ratios when U=5 and R=1. Columns 1, 2 and 3 are c_b=0.1, 0.3 and 0.5 respectively. Rows 1, 2, 3, 4 and 5 are the first, second, third fourth and fifth mode respectively

Next, the beams with different width and thickness taper ratios are discussed. Because the proposed method based on AMDM technique offers a unified and systematic procedure for vibration analysis for the rotating tapered beams. The modification of taper ratios from one case to another is as simple as changing the values of the taper ratios c_b and/or c_h. And it does not involve any changes to the solution procedures or algorithms.

Table 4 illustrates the effect of the taper ratios on the first four natural frequencies when the dimensionless rotating speed U=5 and offset length R=1. From Table 4, it can be found that the first natural frequency increases when the width taper ratio c_b and/or thickness taper ratio c_h increases. However, on the contrary, for the second, third and fourth modes, the thickness taper ratio c_h has an almost linear decreasing effect on the natural frequencies, and the width taper ratio c_b has little influence on the natural frequencies. This conclusion is well agreed with the results in publications (Banerjee *et al.* 2006, Ozdemir and Kaya 2006b). Fig. 3 shows the effect of the taper ratios on the first five mode shapes under different rotating speeds and offset lengths. It can be found that the discrepancies between the mode shapes under different taper ratios become much large with increasing the mode number.

5. Conclusions

In this paper, free vibrations of the rotating tapered cantilever Euler-Bernoulli beams are carried out using Adomian modified decomposition method (AMDM). The advantages of the AMDM are its fast convergence of the solution and its high degree of accuracy. Natural frequencies and corresponding mode shapes with various taper ratio, offset length and rotating speed are presented. Furthermore, the natural frequencies obtained by using AMDM are in excellent agreement with published results. The effects of the offset length, taper ratios and rotating speed on the natural frequencies and corresponding mode shapes are investigated. The numerical results show that the natural frequencies increase with the increase in the offset length and/or rotating speed. The changes of the mode shapes under different rotating speeds become smaller as increasing the modal number. For given rotating speed, the first natural frequency of the tapered beam increases when the width and/or thickness taper ratio increases.

Acknowledgments

This work was sponsored by the National Natural Science Foundation of China (no. 51265037, no. 11464031), Technology Foundation of Jiangxi Province, China (no. KJLD12075), Science Foundation of Educational Committee of Jiangxi Province (no. GJJ13524)

References

Adomian, G. (1994), *Solving frontier problems of physics: The decomposition method*, Kluwer-Academic Publishers, Boston.

Banerjee, J.R. (2000), “Free vibration of centrifugally stiffened uniform and tapered beams using the dynamic stiffness method”, *J. Sound Vib.*, **233**(5), 857-875.

Banerjee, J.R., Su, H. and Jackson, D.R. (2006), “Free vibration of rotating tapered beams using the

dynamic stiffness method", *J. Sound Vib.*, **298**, 1034-1054.
Banerjeea, J.R. and Jackson, D.R. (2013), "Free vibration of a rotating tapered Rayleigh beam: A dynamic stiffness method of solution", *Comput. Struct.*, **124**, 11-20.
Bazoune, A. (2007), "Effect of tapering on natural frequencies of rotating beams", *Shock Vib.*, **14**, 169-179.
Hsu, J.C., Lai, H.Y. and Chen, C.K. (2008), "Free vibration of non-uniform Euler-Bernoulli beams with general elastically end constraints using Adomian modified decomposition method", *J. Sound Vib.*, **318**, 965-981.
Mao, Q. (2011), "Free vibration analysis of multiple-stepped beams by using Adomian decomposition method", *Math. Comput. Model.*, **54** (1-2), 756-764.
Mao, Q. (2012), "Free vibration analysis of elastically connected multiple-beams by using the Adomian modified decomposition method", *J. Sound Vib.*, **331**, 2532-2542.
Mao, Q. and Pietrzko, S. (2012), "Free vibration analysis of a type of tapered beams by using Adomian decomposition method", *Appl. Math. Comput.* **219**(6), 3264-3271.
Mao, Q. (2013), "Application of Adomian modified decomposition method to free vibration analysis of rotating beams", *Math. Probl. Eng.*, Article ID 284720, doi: 10.1155/2013/284720.
Ozdemir, O. and Kaya, M.O. (2006a), "Flapwise bending vibration analysis of a rotating tapered cantilever Bernoulli-Euler beam by differential transform method", *J. Sound Vib.*, **289**, 413-420.
Ozdemir, O. and Kaya, M.O. (2006b), "Flapwise bending vibration analysis of double tapered rotating Euler- Bernoulli beam by using the differential transform method", *Meccanica*, **41**, 661-670.
Rajasekaran, S. (2013), "Differential transformation and differential quadrature methods for centrifugally stiffened axially functionally graded tapered beams", *Int. J. Mech. Sci.*, **74**, 15-31.
Rach, R., Adomian, G. and Meyers, R.E. (1992), "A modified decomposition", *Comput. Math. Appl.*, **23**, 17-23.
Vinod, K.G., Gopalakrishnan, S. and Ganguli, R. (2007), "Free vibration and wave propagation analysis of uniform and tapered rotating beams using spectrally formulated finite elements", *Int. J. Solids Struct.*, **44**(18-19), 5875-5893.
Wang, G. and Wereley, N.M. (2004), "Free vibration analysis of rotating blades with uniform tapers", *AIAA J.*, **42**(12), 2429-2437.

CC